CASL-U-2015-0151-000

SMR Fuel Cycle Optimization and Control Rod Depletion Using NESTLE and LWROPT

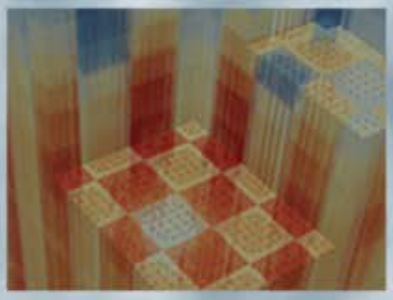

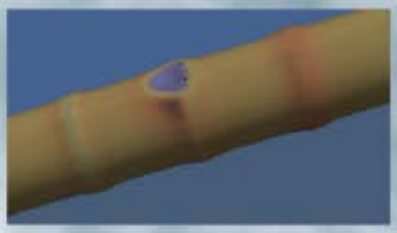

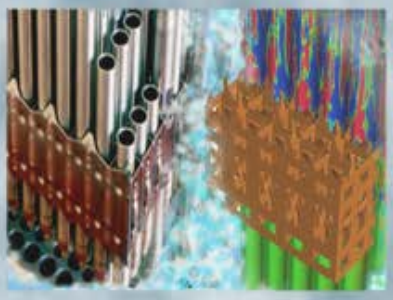

Keith E. Ottinger, P. Eric Collins, Nicholas P. Luciano, and G. Ivan Maldonado
University of Tennessee — Knoxville

March 29, 2015

U.S. DEPARTMENT OF ENERGY | Nuclear Energy
CASL-U-2015-0151-000

Advances in Nuclear Fuel Management V (ANFM 2015)
Hilton Head Island, South Carolina, USA, March 29 - April 1, 2015, on CD-ROM, American Nuclear Society, LaGrange Park, IL (2015)

SMR FUEL CYCLE OPTIMIZATION AND CONTROL ROD DEPLETION USING NESTLE AND LWROPT

Keith E. Ottinger, P. Eric Collins, Nicholas P. Luciano, and G. Ivan Maldonado
The University of Tennessee
Department of Nuclear Engineering
Pasqua Engineering Building
Knoxville, TN 37996-2300
kottinge@utk.edu; pcollin6@utk.edu; nluciano@utk.edu; imaldona@utk.edu

Keywords: NESTLE, LWROpt, Fuel Cycle Optimization, Control Rod Pattern, SMR

ABSTRACT

The multi-cycle BWR fuel cycle optimization code BWROPT has been generalized to handle PWRs and SMRs and renamed LWROpt (Light Water Reactor Optimizer) and an eighth core symmetric shuffle option has also been implemented. The new features of the optimizer are tested using a test case based on an SMR model previously developed manually. Also, preliminary tests of a spatially-dependent and movable-region isotopic tracking feature under development in NESTLE are illustrated with the ultimate goal of assessing control rod depletion for very long SMR rodded cycles.

1. INTRODUCTION

BWROPT[1,2], a multi-cycle BWR fuel cycle optimization code, has been adapted to work with Pressurized Water Reactors (PWRs) and Small Modular Reactors (SMRs). To reflect this change, the code's name has been changed to Light Water Reactor Optimizer (LWROpt). LWROpt performs new fuel inventory and Loading Pattern (LP) optimization using Parallel Simulated Annealing (PSA) by mixing of states[3] and can generate Control Rod Patterns (CRPs) using a heuristic search. Candidate solutions consist of a new fuel inventory, LP, and reactivity control strategy. These solution candidates are evaluated with an updated version of NESTLE[4–6], a 3D, few-group nodal diffusion core simulator, which was developed at North Carolina State University and is currently being enhanced and maintained by the University of Tennessee.

An area of ongoing development in the NESTLE code is the ability to perform isotopic depletion calculations on control rod materials with the ORIGEN module of the SCALE codes suite. The intention of this feature is to enable optimal control rod utilization by accurately determining the remaining absorbing capacity of the rods. BWRs and advanced PWR and some SMR designs rely on control rods/blades for criticality control and power shaping and thus operate at full power with rods inserted. After extended or multiple cycles, the absorbing isotopes in these rods may deplete significantly according to the power and rod pattern history. NESTLE, by coupling to ORIGEN, intends to capture these effects by tracking the concentrations of absorbing nuclides in the control rods throughout the cycle and use that information either with an empirical relationship or to reconstruct the macroscopic absorption cross section of the rod in order to determine the remaining effectiveness of the rod.

CASL-U-2015-0151-000

The SMR design used in this work is based on a previously developed model[7] used to test some of the features of the Virtual Environment for Reactor Applications (VERA) software under development by the Consortium for Advanced Simulation of Light Water Reactors (CASL) at Oak Ridge National Laboratory (ORNL). The core model was developed using design specifications and criteria from publications based on an actual SMR under development[8,9].

2. METHODOLOGY

2.1. Loading Pattern and New Fuel Type Optimization

The LP and new fuel inventory optimization methodology used in LWROpt has been described in detail in previous publications[1,2] so only a brief overview and recent improvements are included here. The PSA optimization algorithm is used to control the acceptance of solution changes which can be made via the 11 user selectable solution change types. These change types include three shuffles, seven new fuel type changes, and the latest addition a rotation change (a type of shuffle), which is used to determine exposed assembly placement for symmetric assemblies when the eighth core shuffle option is used. The new fuel types available for use in an optimization can be organized into an array of up to four dimensions with the option of limiting new fuel type changes to only nearest neighbors in the array.

Candidate solutions are compared with an Objective Function (OF) that has the following user selectable components/constraints: Fuel Cycle Cost (FCC), minimum k_{eff}, maximum k_{eff}, maximum 2D (assembly) Relative Power Fraction (RPF), maximum 3D (node) RPF, maximum 2D exposure, and maximum 3D exposure. There are four methods available for depleting candidate solutions: user input depletion steps and CRP, performing a CRP search with user input depletion steps, a one-step Haling depletion[10], and an All Rods Out (ARO) depletion with user input depletion steps. Additional recent improvements include the ability to shuffle less than full-core PWR and SMR models that use more than one radial node per assembly, and an eighth core symmetric shuffle option that works with all LWR models.

2.2. Control Rod Pattern Search

There are two automated heuristic CRP search methods in LWROpt as well as a manual CRP search option. The objective of the two automated CRP search algorithms is to find a long term (1-2 GWD/MTU steps) CRP that meets the 2D RPF, 3D RPF, and the upper and lower k_{eff} limits. The two methods are named based on their level of complexity: simple and complex. The simple automated CRP search is intended to be used for depleting candidate LPs during a new fuel and LP optimization and, consequently, has minimal move checking and conflict resolution to reduce runtime. This algorithm selects which Control Rod (CR) to move based on which CR group's Region Of Influence (ROI) has the largest constraint violations or greatest margin depending on whether k_{eff} is greater than or less than the average of the upper and lower k_{eff} limits, respectively. The ROIs of a CR as defined elsewhere[11,12] are shown graphically in Fig. 1 with the nodes directly affected by the CR referred to as Control Cell (CC) nodes. For BWRs each box in the figure is an assembly and the CRs (actually control blades) are cruciform shaped as depicted. For PWRs/SMRs each box is a

CASL-U-2015-0151-000

node (assemblies are modeled radially as a 2x2 grid of nodes) and the CRs consist of many small rods that are inserted into the assembly via guide tubes, but the cruciform depiction is used for simplicity.

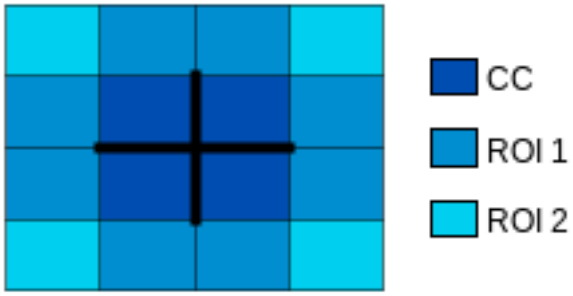

Fig. 1. Locations of the control rod regions of influence.

The complex automated CRP search is more thorough with significant move checking and therefore longer runtimes than the simple method. Because of this the complex search is useful mostly for generating CRPs for individual LPs and new fuel and LP optimizations in which a CRP search is performed infrequently. The complex method uses the average constraint violation weighted distance from each fuel location to each CR to decide which CR group to move. The manual CRP search can be used by itself or the user can run an automatic search and choose to have the search switch to manual if the automatic search does not find a CRP that meets all of the constraints for a depletion step.

2.3. Small Modular PWR Model

A non-proprietary small PWR core was developed using available open literature. The modularity of the design was to be achieved in part by using a single four-year cycle, although alternative multi-cycle shuffle-core designs have also been considered[9]. The design specifies the non-use of soluble poisons such as boron, therefore primary reactivity control is achieved through the movable Ag-In-Cd (AIC) control rods. This method of reactivity control demonstrates the strong motivation for optimizing the CRPs and tracking the CR depletion through the cycle.

The core consists of 69 fuel assemblies each using a standard 17x17 pin lattice on a 21.5 cm pitch. The total assembly height is 241.3 cm, which includes upper and lower axial reflector regions each 10.16 cm in height. The lattice includes 24 control rodlet locations, and one central instrument tube. All other pin locations were available in the design for fuel rods or burnable poison rods (BPRs). The model before optimization will be referred to as *the baseline design*. The baseline design used four lattice types, each with a different number and configuration of burnable poisons. To achieve the four year cycle length, the standard UO2 fuel pin is a relatively high 4.95% enrichment. Integral burnable poisons (UO2-Gd2O3) and BPRs (B4C-Al2O3) are used in the lattices to reduce maximum relative pin power peaking to ≤ 1.1. The UO2-Gd2O3 pins use a reduced enrichment of 3.95% and contain 3.0% Gd2O3 by

weight. The BPRs contain 4.0% B4C by weight. The upper and lower axial reflector regions contain natural uranium in the UO2 and UO2-Gd2O3 pin locations and a zirconimum-water mixture in the BPR locations.

The baseline core design was eighth symmetric using four assembly types, one for each lattice type, with no axial variation in the active fuel region. Assemblies with the greatest number of burnable poison pins were placed generally in the core's interior and those with fewer near the core periphery. Fig. 2 shows the assembly configuration, and Table 1 shows the lattice parameters for each assembly. The core power is 440 MWt, with a baseline fuel temperature of 840 K, inlet coolant temperature of 570 K and flow rate of 30 Mlbm/hr.

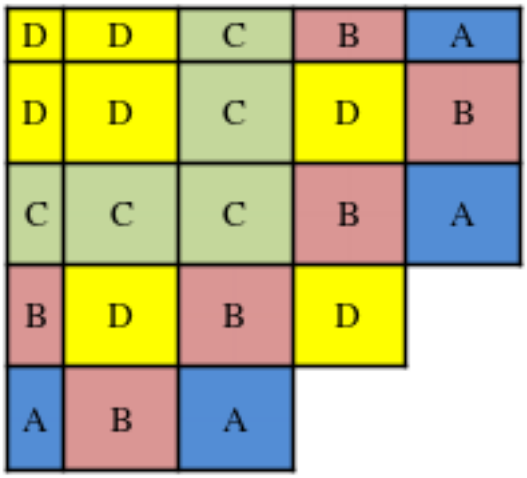

Fig. 2. Baseline design loading pattern.

Table 1. Lattice parameters used in the baseline SMR design.

Assembly Type	Standard Fuel Pins # / Enrichment	Gd2O3 Fuel Pins # / Enrichment (Weight%)	B4C BPRs # (Weight%)
A	248 / 4.95%	4 / 3.95% (3.0%)	12 (4.0%)
B	244 / 4.95%	4 / 3.95% (3.0%)	16 (4.0%)
C	240 / 4.95%	4 / 3.95% (3.0%)	20 (4.0%)
D	236 / 4.95%	4 / 3.95% (3.0%)	24 (4.0%)

To test the SMR optimization capability of LWROpt the new fuel inventory and LP for the first cycle of this SMR were optimized using the ARO step depletion with a depletion step size of 2 GWD/MTU. Only the first cycle was optimized because the four year cycle is intended to require a completely new core for each cycle instead of only replacing part of the

fuel as is typically done. The optimization was performed with a quarter-core model and the eighth core shuffle option to replicate the symmetry of the baseline design. The cycle energy production was set to 1400 EFPD (4 years of operation with a 95% capacity factor)[8]. The constraints used for the LP and CRP optimizations are listed in Table 2. The k_{eff} limits are based on the need to maintain criticality. The maximum k_{eff} limit was only used for the CRP search and was set to allow for a small range of acceptable values to generate CRPs that can be made critical with small manual adjustments. The node RPF limit was taken from one of the papers used to develop the SMR model[8] and the assembly RPF was set to a reasonable limit but did not affect the final results much. Assembly and node exposure limits were used but because of the low burnup of the cycle and lack of reloading used fuel in later cycles they were not significant.

Table 2. Constraints used for LP and CRP optimizations.

Constraint	Limit
Minimum k_{eff}	1.000
Maximum k_{eff}	1.001
Maximum 2D RPF	1.6
Maximum 3D RPF	2.0

The complex CRP search was used to generate CRPs for several of the best LPs found to determine the best overall new fuel inventory and LP. The CRs were split into two banks which along with the CR group locations are shown in Fig. 3. Because of the reduced height of the SMR core only 20 axial fuel nodes were used in the NESTLE model so the CRP search used 40 notches with every other notch falling on a node boundary and being usable.

2.4. Control Rod Depletion

The implementation of control rod depletion capabilities in the NESTLE code has occurred in three phases. NESTLE has been coupled to SCALE-ORIGEN for depletion of materials that remain stationary within the core. The methodology of using microscopic cross sections and few group flux disadvantage factors to deplete these materials has been described elsewhere[13]. This was the first step, from which depletion of movable control rod materials is an extension.

The next step required NESTLE to track the shifting locations of control rod materials throughout the fuel cycle and treat cross sections appropriately at each burnup step based on the rods' local surroundings. Tracking of the control rod materials has been implemented in such a way as to allow the user as much flexibility as possible (or as little as desired) in defining the control rod material boundary. To achieve this in an organized fashion, a tiered scheme is used. At the top level, control rods/blades are grouped into banks. Every control rod in a common bank is assumed to have identical physical dimensions and

CASL-U-2015-0151-000

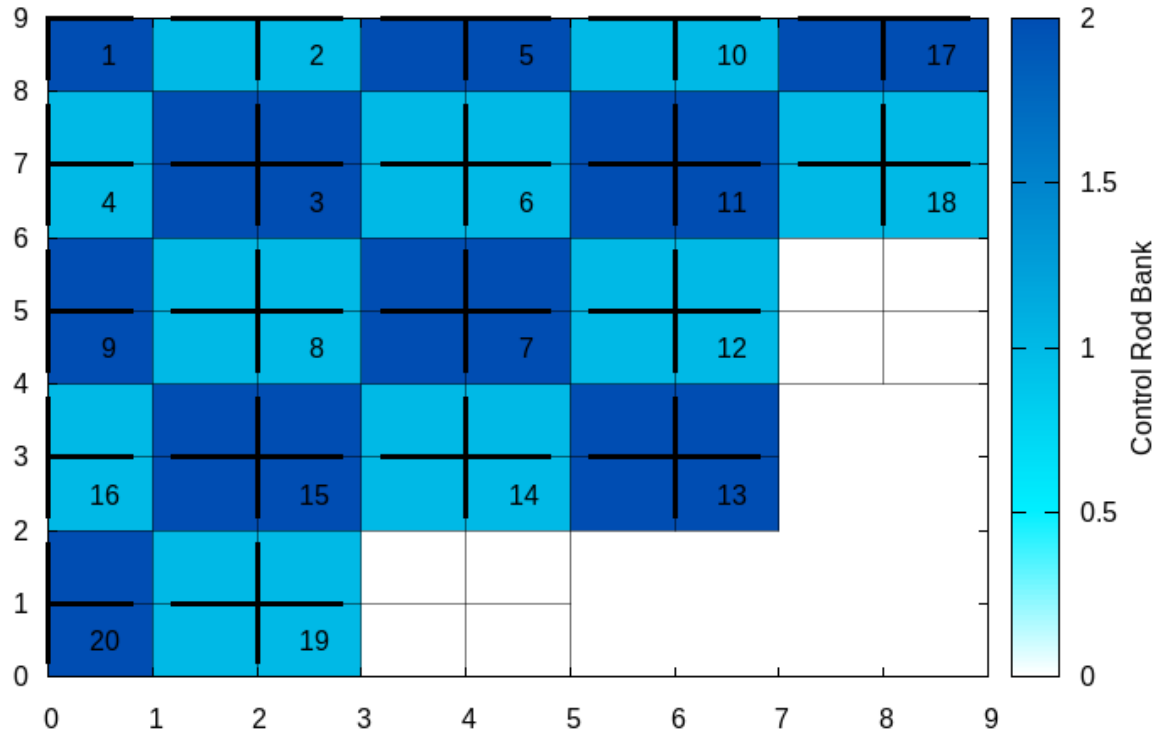

Fig. 3. Control rod bank and group locations.

movements throughout the cycle. Within a bank is a user-defined number of control rod assemblies. These represent physical control blades (BWRs) or control rod clusters (PWRs). Control assemblies can be further divided into sub-assemblies, if appropriate, which are abstract subdivisions corresponding to planar nodes from the nodal discretization of the core geometry. For example, a typical PWR nodal discretization would be to divide fuel assemblies into quadrants, so the control sub-assembly would be the collection of elements within that quadrant. A control sub-assembly contains an arbitrary number of 'elements,' which represent individual control pins/rodlets within the cruciform (BWRs) or rod cluster (PWRs). An element may be further divided into a user-defined number of radial, concentric 'regions,' or rings. This enables NESTLE to properly capture the 'skin effect' of control rod depletion[14]. Finally, each region is divided axially into a number of 'exposure nodes,' which are characterized by unique materials and are depleted individually. The term 'exposure node' has been used in other work related to control rod depletion[15]. The size, distribution, and number of geometric divisions are at the user's discretion and will depend on the intended application.

Exposure nodes are expected to move axially into different fuel nodes at various points throughout the fuel cycle. In fact, depending on its length relative to that of a fuel node and the bank's withdrawal position, an exposure node may even span multiple fuel nodes at a single depletion step. For this reason, it is necessary to obtain microscopic cross sections (to use in depletion) for an instance of a control rod exposure node material in potentially several fuel lattice types which may house the exposure node at a given time. This cross section

data becomes a component of the exposure node data structure, and is used to facilitate the depletion when appropriate.

Following the depletion calculation, the user may request the depletion results for an individual exposure node, or may construct a component average using the results from multiple regions, elements, sub-assemblies, assemblies, and banks. Clearly, this structure enables very detailed models of control rod depletion, for which component (such as sub-assembly or assembly) averages of the depletion results would be necessary to manage and comprehend them. For example, within a single sub-assembly, a user could choose to model a dozen elements individually, dividing each into six regions, and dividing the rod axially into several exposure nodes. With this approach, spatial effects of depletion would be well captured, but extensive, detailed input would be required, and run times would be long. Alternatively, a user may choose to model just one element per sub-assembly to represent a homogenized average of all control pins, one region per element, and merely a couple axial exposure nodes. While less accurate, this is a much simpler way to use the same scheme.

The last phase of implementing this feature involves the processing and application of the depletion results to provide an assessment of rods' remaining absorbing capacity. This phase is still under development. A first approach to accomplishing this task may be to apply an empirical model based on the factor of reduction in the absorbing isotopes' concentrations. Ultimately, it is envisioned that this depletion calculation will contribute to a microscopic cross section model within NESTLE and serve to capture not only the depletion of control rods, but also the effect of depleting control rods on the fuel cycle.

3. RESULTS

3.1. Optimized New Fuel Inventory, Loading Pattern, and Control Rod Pattern

The constraint values for the baseline design and the best solution found during the LP search are given in Table 3. LWROpt was able to eliminate the insufficient reactivity and node RPF constraint violations present in the baseline design. It should be noted that these values are for ARO and that the RPF values are therefore not necessarily what would be seen in actual operation. The best overall LP found during the LP and CRP searches is shown in Fig. 4. The distribution of the fuel types is somewhat similar to the baseline design with the least reactive fuel in the center and the most reactive on the outside. However, there is much more type A fuel leading to no variation in the fuel in the outer ring. This increase in type A fuel was likely driven by the insufficient reactivity of the baseline design. If ShutDown Margin (SDM) was considered (there is currently not a quick method of calculating this in NESTLE or LWROpt) the outer ring would likely have to be more diverse because the two corner assemblies do not have CRs.

Constraint values for the depletion of the best LP with the CRP found during the CRP search are plotted for each of the depletion steps in Fig. 5. As can be seen there were constraint violations for all of the constraints though only a very minor violation for assembly RPF. The value of k_{eff} oscillates between high (+600 pcm) and low (-400 pcm) values early in the cycle then settles into a smaller range a little above critical. The node RPF was less than 120% of the limit for the first half of the cycle and roughly equal to or less than the limit afterwards.

Table 3. Constraint values for the baseline and best LPs for the ARO depletion.

Constraint	Limit	Baseline	Best
Minimum k_{eff}	1.000	0.9983	1.0037
Maximum 2D RPF	1.6	1.53	1.40
Maximum 3D RPF	2.0	2.400	1.998

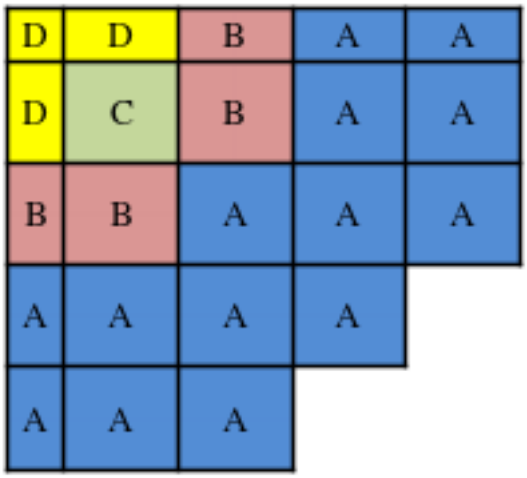

Fig. 4. Best loading pattern found by LWROpt.

The CRPs generated at each depletion step are shown in Fig. 6. Early in the cycle bank two required most of the CRs to be fully inserted and still was not able to meet the keff limits while bank one had excess worth. Comparing the constraint violation plots and the CRPs reveals that two of the three highest k_{eff} values coincided with bank two being fully or nearly fully inserted. The highest assembly and node RPF values coincided with the second highest k_{eff} value indicating the peaking would be worse for a critical core. The inability of bank two to meet the k_{eff} limit indicates the LP will need to be adjusted because bank two does not have enough worth in the outer region to suppress the reactivity of the ring of type A fuel. This data also points to the need for the ability to use alternate banks when the primary bank is not capable of meeting constraints which will be added to LWROpt (this will also help with power shaping). Also the core k_{eff} is slightly more than 1.0 at EOC and the there are still CRs inserted which was also seen in the EOC k_{eff} from the LP optimization and indicates that there is excess reactivity in the new fuel. This could be caused by the small number of assemblies in the eighth core shuffle and the gap in the reactivity of the available assembly types or it could also indicate the need for feedback between the LP and CRP searches.

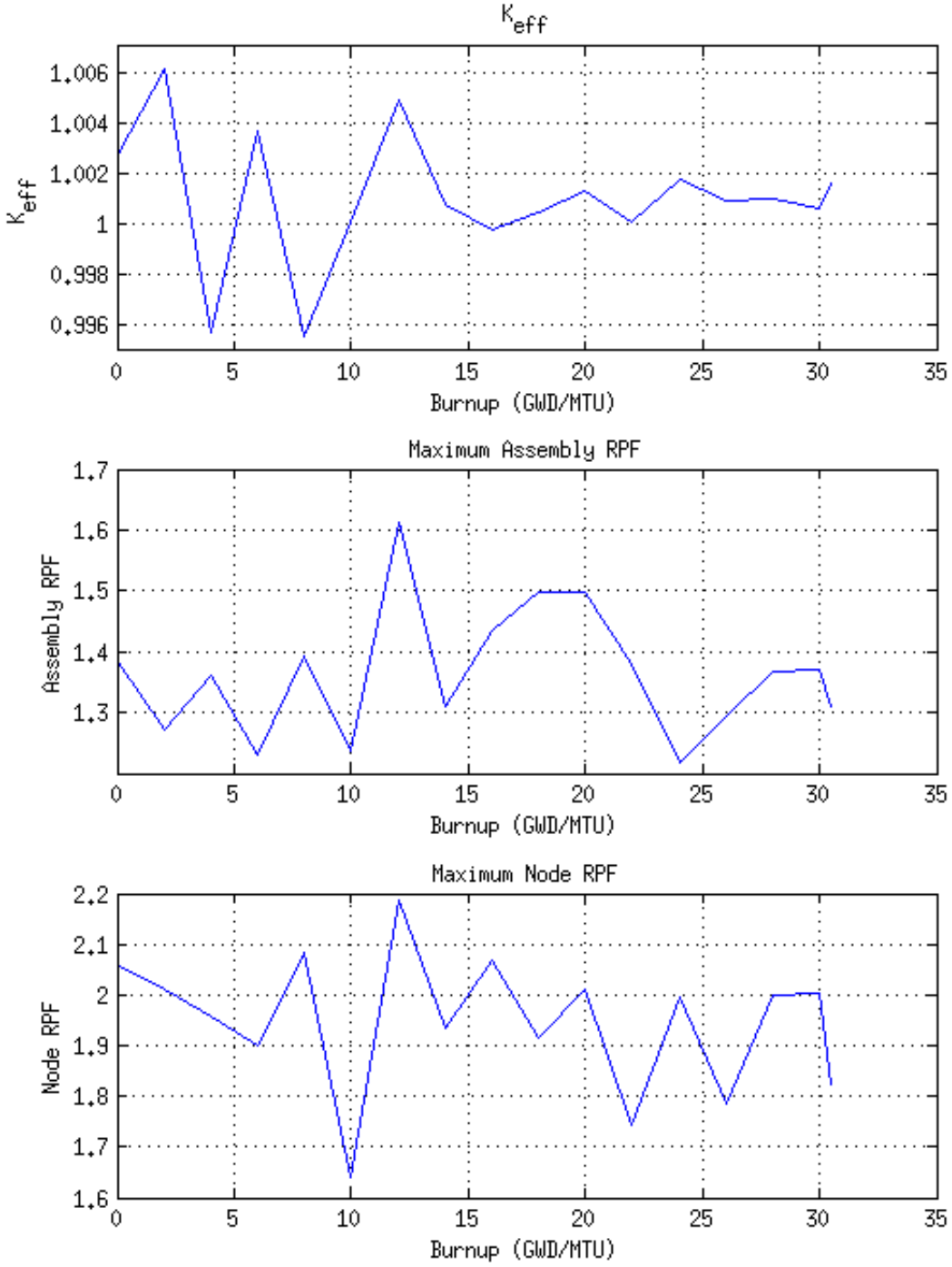

Fig. 5. Constraint values as a function of burnup for best LP/CRP.

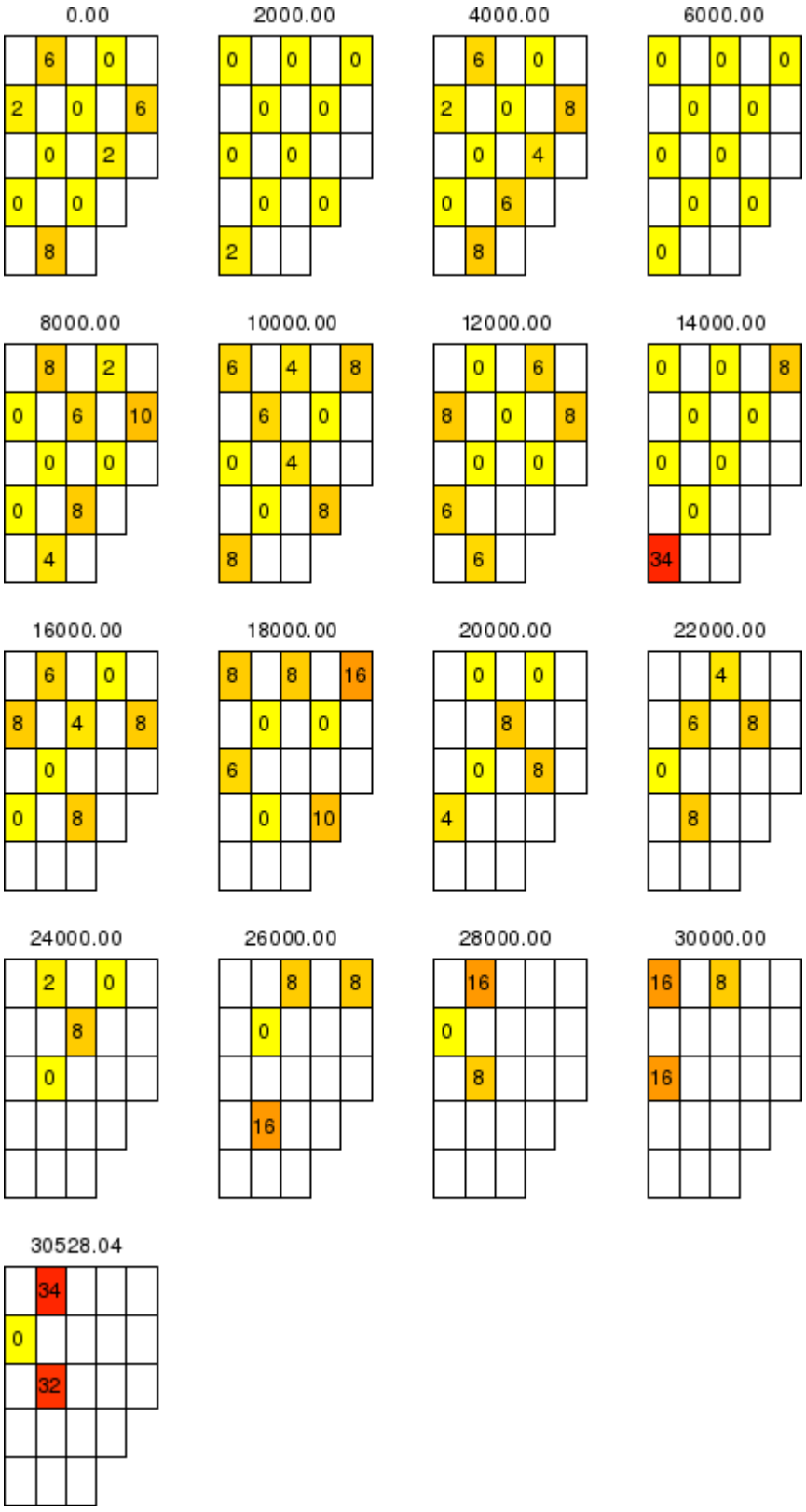

Fig. 6. Control rod patterns generated for the best LP (notches withdrawn, 40 total notches).

3.2. Control Rod Depletion

To illustrate NESTLE's control rod depletion capability in its current stage of development, a demonstration calculation was performed which models a single, simplified fuel bundle from the previously described SMR design with incrementally receding AIC control rods. In order to isolate the effect of depleting control rods, this calculation employed a *frozen fuel* model, in which fresh fuel is assumed throughout the calculation and only control rod materials are depleted. The model specified radially reflective boundary conditions and used top and bottom axial reflector nodes consisting of 20 cm of coolant. For the purpose of this demonstration, the single assembly's rod cluster was artificially divided into two banks so that the assembly could have control rods in different positions. The two control rod banks are assigned in a checkerboard pattern. The first rod bank was fully inserted initially and was withdrawn at 50 day increments until it was fully withdrawn after 1400 days, the approximate length of the fuel loading cycle. The second rod bank was fully withdrawn throughout the entire calculation in order keep the model somewhat closer to critical. The second rod bank was not depleted. The first rod bank included two sub-assemblies, each with one element divided equally into six radial regions and four axial exposure nodes.

The output of the depletion calculation provides isotopic concentrations for all of the significant nuclides in every control rod material and at each depletion step. For exposure node 1, corresponding to the bottom fourth of the control rod, the atom density of Ag^{109}, a major absorber, in each of the six regions is shown in Fig. 7. This figure illustrates the

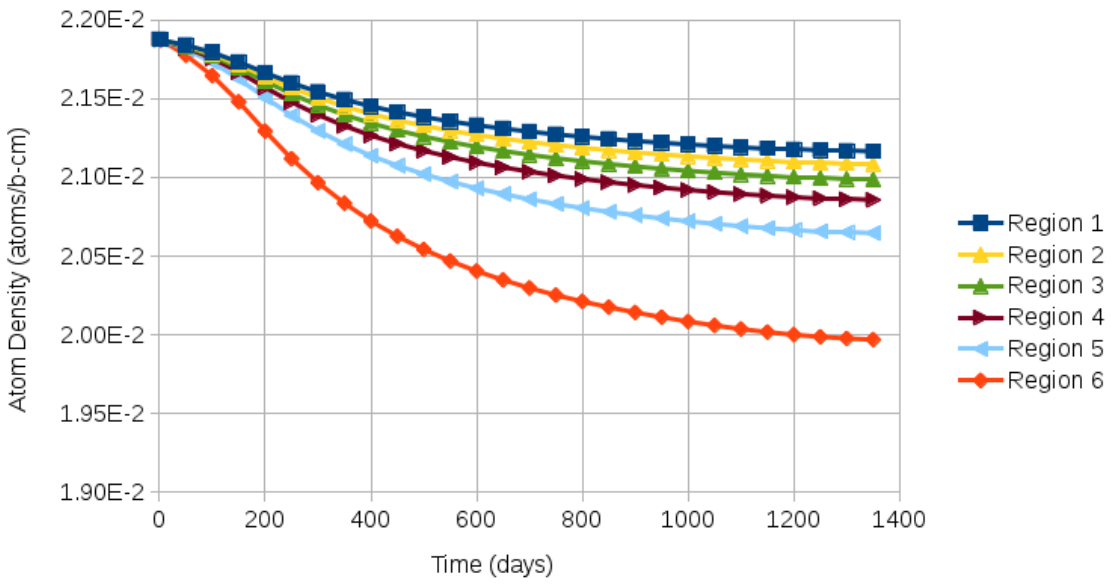

Fig. 7. Depletion results for Ag^{109} in exposure node 1 by region. Regions are concentric annular volumes in the control rodlet, with region 6 the outermost, and region 1 the innermost.

skin effect in that the outer region material (region 6) depletes much more quickly than the inner regions. This pattern is observed for all of the significantly absorbing nuclides and all

exposure nodes. Fig. 8 shows the element-average concentration of Ag^{109} in each of the four exposure nodes. The element-average concentration for an isotope is the volume-weighted average of all the regions within an element. This plot reflects the withdrawal of the control

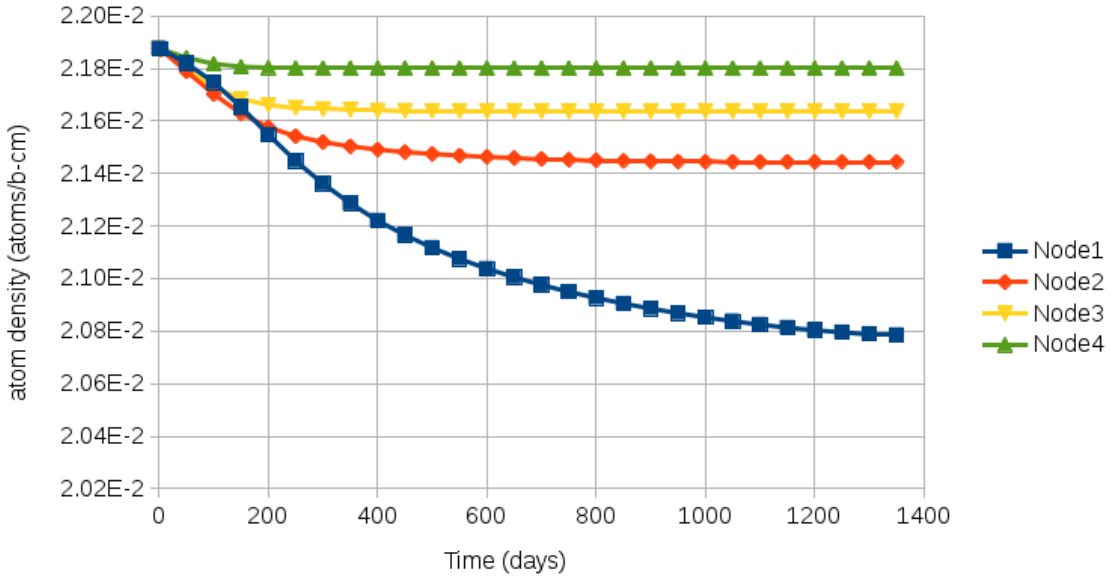

Fig. 8. Depletion results for Ag^{109} in each exposure node. Exposure node 1 is bottom of the control rod, and exposure node 4 is the top.

rod, as each exposure node only depletes for the time that it is inserted into the fuel. Exposure node 4, which is the top and the first exposure node to exit the fuel bundle, depletes only for the first few intervals. Exposure node 1, the tip of the control rod, depletes during all of the intervals. Also, being at the tip and most near to where the neutron flux is highest, exposure node 1 depletes much more quickly than other exposure nodes present in the core. The results of this calculation demonstrate proof of concept and functionality of control rod depletion in NESTLE but have yet to be verified or validated. A comparison of depletion results to an identical model using a three dimensional Monte Carlo code is currently being conducted.

4. CONCLUSIONS

The LP optimization in LWROpt was able to find an eighth symmetric LP for the SMR model that met all of the constraints specified. However, the CRP search was not able to find a satisfactory CRP for the optimized LP. The failure of the CRP search was at least partially the result of the LP optimization, which was performed using a stepped ARO depletion, not taking into account the limitations of reactivity control with the CR banks. This is the reason performing a coupled LP/CRP optimization or at least having feedback between the two is the best approach for this type of optimization and will be the next step in the SMR optimization.

Results from the control rod depletion calculation with NESTLE demonstrate a feature under development with the potential to provide the unique capability of accurately capturing

history effects in depletion of control rods. Although this work is ongoing, the demonstration shows that the feature is in working condition and provides a "proof of concept" for the approach. Work will continue in this area with independent code-to-code verification of NESTLE results and the development of a feedback mechanism in order to quantify the effect of depleting control rods on the fuel cycle.

5. ACKNOWLEDGEMENTS

We would like to acknowledge Kelly Kenner, formerly with the University of Tennessee and currently with the Tennessee Valley Authority, for her work with the SMR design. We would also like to acknowledge the helpful advice of Gary Galloway.

REFERENCES

1. Ottinger, K., Maldonado, G. I., "Multi-Cycle Boiling Water Reactor Fuel Cycle Optimization," *Proc. Global 2013*, Salt Lake City, UT, September 29-October 3, American Nuclear Society (2013).

2. Ottinger, K., "Multi-Cycle Boiling Water Reactor Fuel Cycle Optimization," PhD Dissertation, University of Tennessee Knoxville (2014).

3. Chu, K.-W., Deng, Y., Reinitz, J., "Parallel Simulated Annealing by Mixing of States," *Journal of Computational Physics*, **148**, 646-662 (1999).

4. Turinsky, P., Al-Chalabi, R., Engrand, P., *et al.*, "Code Abstract - NESTLE: A Few-Group Neutron Diffusion Equation Solver Utilizing the Nodal Expansion Method for Eigenvalue, Adjoint, Fixed-Source Steady-State and Transient Problems," *Nuclear Science and Engineering*, **120**, 72 (1995).

5. Galloway, J., Hernandez, H., Maldonado, G. I., *et al.*, "BWR Modeling Capability and SCALE/TRITON Lattice-to-Core Integration of the NESTLE Nodal Simulator," *Proc. PHYSOR 2010*, Pittsburgh, PA, May 9-14, American Nuclear Society (2010).

6. Luciano, N. P., Ottinger, K. E., Collins, P. E., *et al.*, "The NESTLE 3D Nodal Simulator: Modern Reactor Models," *Proc. M&C 2015*, Nashville, TN, April 19-25,American Nuclear Society, to appear.

7. Kenner, K. R., Montgomery, R., Maldonado, G. I., "Modeling an iPWR Startup Core Cycle with VERA," *Trans. Am. Nucl. Soc.*, Vol. 111, p. 1388-1390, American Nuclear Society (2014).

8. Erighin, M., "A 48-Month Extended Fuel Cycle for the B&W mPower^{TM} Small Modular Nuclear Reactor," *Proc. PHYSOR 2012*, Knoxville, Tennessee, April 15-20, American Nuclear Society (2012).

9. Scarangella, M., "An Extended Conventional Fuel Cycle for the B&W mPower^{TM} Small Modular Reactor," *Proc. PHYSOR 2012*, Knoxville, Tennessee, April 15-20, American Nuclear Society (2012).

10. Haling, R. K., "Operating Strategy for Maintaining an Optimum Power Distribution Throughout Life," US Atomic Energy Commission, TID-7672, (1964).

11. Lin, L. S., Lin, C., "A Rule-Based Expert System for Automatic Control Rod Pattern Generation for Boiling Water Reactors," *Nuclear Technology*, **95**, 1-8 (1991).

12. Karve, A.,Turinsky, P., "FORMOSA-B: a Boiling Water Reactor In-Core Fuel Management Optimization Package II," *Nuclear Technology*, **131**, 48-68 (2000).

13. Collins, P. E., Luciano, N., Maldonado, G. I., "Modernization and Expansion of Isotopic Depletion Capabilities within the NESTLE 3D Nodal Simulator," *Trans. Am. Nucl. Soc.*, Vol. 111, pp. 1230-1233, American Nuclear Society (2014).

14. Collins, P. E., Luciano, N., Maldonado, G. I., "Parametric Study to Capture the Skin Effect in PWR Control Rod Depletion," *Trans. Am. Nucl. Soc.*, Vol. 119, pp. 1327-1329, American Nuclear Society (2013).

15. Franceschini, F., Zang B., Mayhue, L., *et al.* "Development of a control rod depletion methodology for the Westinghouse NEXUS system" *Progress in Nuclear Energy*, **68**, 235-242 (2013)